Fluorescence enhancement mechanism in phosphor $CaAl_{12}O_{19}:Mn^{4+}$ modified with alkali-chloride

Yanan Li[1], Zunhong Xiao[1], Lizhi Xu[1], Yingping Zou[2], Mingchun Guo[3]

[1]*School of Chemistry and Materials Science, Guizhou Normal University, Guiyang 550001, People's Republic of China*
[2]*School of Chemistry and Chemical Engineering, Central South University, Changsha 410083, People's Republic of China*
[3]*School of Chemistry and Materials Science, University of Science and Technology of China, Hefei 230026, People's Republic of China*
E-mail: xzh729@126.com

Published in Micro & Nano Letters; Received on 23rd October 2012; Revised on 28th February 2013; Accepted on 1st March 2013

$CaMAl_{12-x}O_{19}:xMn^{4+}$ (M is one or more of K^+, Na^+, Li^+) materials were prepared by a combustion method in air atmosphere. The Mn concentration, the influence of one or more alkali-chloride on luminescence properties, crystal phases and surface morphology of the samples were investigated. The fluorescence intensity of $CaAl_{11.98}O_{19}:0.02Mn^{4+}$ modified by combining three kinds of alkali-chloride can be enhanced by three times. Blue shift of $CaMAl_{12-x}O_{19}:xMn^{4+}$ luminescence is explained from the point of view of enhancing electron cloud deformation after doping. Alkali metal ions were beneficial to form hexagonal $CaAl_{12}O_{19}$ while there was certain inhibition to other peak strengths. The mechanism is the coexistence of alkali-chloride replacing Al^{3+} or Ca^{2+} instead of Mn^{2+} based on the difference of cation radius, this would increase the luminous centre of Mn^{4+} and provide charge compensation at the same time. The size of red phosphors was 5–10 μm, which is useful for light emitting diode applications.

1. Introduction: Crystals doped with rare-earth or transition-metal ions are promising photonic sources owing to their applications in high-brightness light emitter devices (HB-LEDs) and the relevant industries such as lasers and other displays. HB-LEDs, especially Ga(In)N-based white LEDs, have the potential to replace traditional incandescent and fluorescent lamps because of their favourable characteristics, such as long lifetime, energy saving and environmental protection [1]. There are generally three systems to generate white LEDs: (i) mix red, green and blue lights emitted by different chips. (ii) combine a blue LED with yellow phosphor materials. (iii) mix lights emitted by red, green and blue phosphor with UV LEDs. The most common method to generate white LEDs for solid-state lighting is to combine a blue LED with yellow phosphor, such as $(Y_{1-a}Gd_a)_3(Al_{1-b}Ga_b)_5O_{12}:Ce^{3+}$ (YAG:Ce) [2–4]. However, the commercialised white LED combining a blue LED with YAG:Ce^{3+} results in poor colour rendering index (CRI) for the lack of the red component in the spectrum. The red phosphors doped with Eu^{3+} are commonly used for conventional lighting owing to their high efficiencies and colour purities. However, the shape absorption peaks originating from f–f transition of Eu^{3+} in UV and blue regions limit their application in current white GaN-based LEDs [5]. Another red phosphor, such as Mn^{4+} doped with $3.5MgO{\cdot}0.5MgF_2{\cdot}GeO_2$ (MFGO), is available to improve the colour rendering of the fluorescent lamps. However, the high cost of GeO_2 limits its wide application [6]. New red phosphors need to be developed because of the increasing demand for economically viable phosphor materials.

$CaAl_{12}O_{19}$ (CAO) doped with Mn^{4+} is a red phosphor identified with a broad absorption band in the visible region and superior chromaticity in the deep red region [7]. The extranuclear electron of Mn^{4+} is $1S^22S^22P^63S^23P^63d^3$, which make Mn^{4+} easy to deformation [8]. So, the red fluorescence peak position and chromaticity can be controlled by the matrix composition. As recently reported, a remarkable enhancement of the luminescent efficiency of $CaAl_{12}O_{19}:Mn^{4+}$ phosphor has been achieved by composition modification through mixing with MgO [9]. But, the effects of different cationic radius and alkali cation synchronous substitution of CAO:Mn has not been investigated. Based on the above considerations, we synthesised red phosphor $CaMAl_{12-x}O_{19}:xMn^{4+}$ and studied the properties of obtained samples. The reason for the effect of combined alkali cations on relative fluorescence intensity and structural properties were discussed in detail in terms of charge compensation and ion deformation theory [10].

2. Experimental

2.1. Materials and methods: The precursors were prepared by using the chemical co-precipitation method. The raw materials used for preparing $CaAl_{12-x}O_{19}:xMn^{4+}$ red phosphors are as follows: calcium nitrate ($Ca(NO_3)_2{\cdot}4H_2O$), aluminium nitrate ($Al(NO_3)_3{\cdot}9H_2O$), manganese chloride ($MnCl_2{\cdot}4H_2O$), potassium chloride (KCl), lithium chloride (LiCl) and sodium chloride (NaCl) (all chemicals were of 99.9% purity). A series of all the raw materials were prepared in deionised water and mixed at appropriate proportions. Then they were precipitated in ammonium bicarbonate (NH_4HCO_3) by the inverse titration method under continuous stirring. The carbon dioxide released during the reaction made the deposition more uniform. Next, add different alkali-chloride whose amounts were 10% of Mn. Then they were heated in an oven at 120°C for 2 h in air to produce a pink, crispy and loosely connected powder. Finally, they were grinded and fired subsequently in a corundum crucible at 1450°C for 3 h in ambient air.

2.2. Characterisation and measurements: Fluorescence measurements were carried out at room temperature using a Hitachi F-4600 spectrofluorimeter with xenon light as the excitation source in the ranges of 500–800 and 300–550 nm, respectively. The excitation and emission slit were 5 nm, which did not change from samples to samples. The powder X-ray diffraction (XRD) study was performed on a Philips X-ray diffractometer with graphite monochromatised Cu Kα radiation ($\lambda = 0.15418$ nm) in the 2θ range of 10–70°. The particle size and surface morphology of the samples were determined by a JSM-6490LV scanning electron microscope (SEM).

3. Results and discussion: The relative fluorescence intensities of $CaAl_{12-x}O_{19}:xMn^{4+}$ phosphors as a function of Mn concentration are shown in Fig. 1. The typical fluorescence emission peaks of $CaAl_{12-x}O_{19}:xMn^{4+}$ phosphors were observed at 578, 645, 653,

doi: 10.1049/mnl.2012.0809

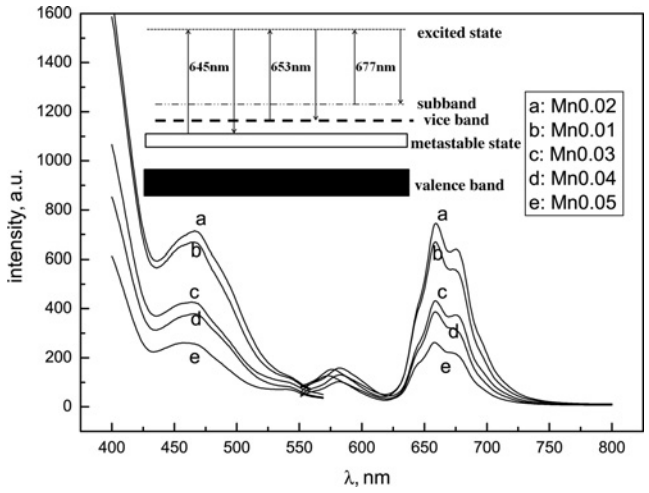

Figure 1 *Fluorescence excitation and emission spectrum of $CaAl_{12-x}O_{19}$: xMn^{4+} under the 458 nm excitation wavelength as a function of Mn concentration*

677 nm wavelength under 460 nm (blue bands) excitation wavelength. It is reported that the main emission peak appeared at 653 nm wavelength due to the $^2E \rightarrow {}^4A_2$ transition of Mn^{4+} ion. The emission band in the 550–580 nm region is due to lattice vibronic transitions of Mn^{4+}, which is much weaker in comparison with the main emission [10]. We explain the reason for forming the multi-emission peak by ion deformation theory [8]. The electrons of the ground state obtain high energy through deformation-induced force. The electrons of manganese will split the metastable states into disparate levels (vice band and sub-band as shown in Fig. 1) when they pass through the valence band due to their different energies at ground state. The electrons will occupy different areas where they emit light with three power densities (645, 653, 677 nm). The numerous electron cloud densities increase in the vice band and thus makes the strongest fluorescence at the 653 nm wavelength. The experiment determined that the Mn^{4+} concentration increases the emission intensity. The main emission intensity at 653 nm with Mn^{4+} concentration of 0.02 mol was the highest among the various Mn concentrations in $CaAl_{12}O_{19}$:Mn^{4+} phosphors due to the increasing number of luminous centres. However, when the Mn^{4+} concentration increased over a certain value ($x = 0.02$) the launch strength declined, because when the activator concentration increased to a certain degree, the unit cell became more symmetrical, and the deformation force is too weak to motivate electrons to go through the valence band, resulting in the electron failing to enter into the metastable state in accordance with characteristic concentration quenching.

Table 1 Radius for all cations in $CaMAl_{11.98}O_{19}$:$0.02Mn^{4+}$

Ion	Charge	Coordination	Ionic radius, nm
Al	3	VI	0.535
Mn	4	VI	0.53
		VI	0.83
		XII	0.90
Ca	2	VI	1.00
		VII	1.06
Li	1	VI	0.76
Na	1	VI	1.02
		VII	1.12
K	1	VI	1.38
		VII	1.46

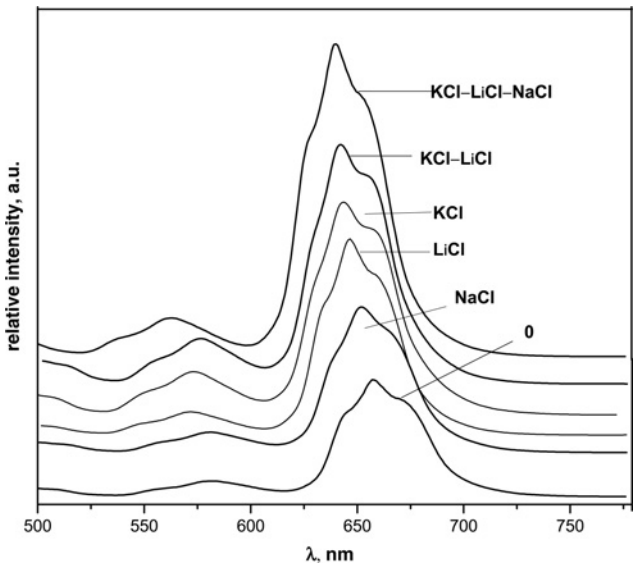

Figure 2 *Fluorescence emission spectra of $CaMAl_{11.98}O_{19}$:$0.02Mn^{4+}$ with the kinds of alkali-chloride from 0 to 3*

Cationic radius is shown in Table 1 [11]. The ion radius of Mn^{4+} is close to Al^{3+}, which accounts for a large share in cationic lattice. Thus, the majority of Mn^{4+} replaces the vacancy formed by Al^{3+}. A part of Mn ions would have to form a Mn^{2+} valence state to make charge compensation. The ion radius of Mn^{2+} (0.080 nm) is nearer to Ca^{2+} that provides conditions for Mn^{2+} to displace Ca^{2+}. This would make Mn^{4+} to easily convert into Mn^{2+}, which would have a certain influence on the luminescence of Mn^{4+}. The filled outermost layer s^2p^6 orbit of alkali metal ions is extremely difficult for achieving deformation. So, the electron of the outermost layer cannot go through the valence band, let alone form a new level in a forbidden band. On the one hand, we chose alkali metal-ions to join in, so that they can replace Mn^{2+} to offset the effects on Mn^{4+} to a certain degree. On the other hand, adding low-valence alkali metal cation was necessary for Mn^{4+} charge compensation and thus made the crystal field more stable.

Fig. 2 shows the fluorescence spectra of $CaAl_{12}O_{19}$:$0.02Mn^{4+}$ phosphors for the function of one or more alkali metal cations. The combined use of three alkali-chlorides showed the highest

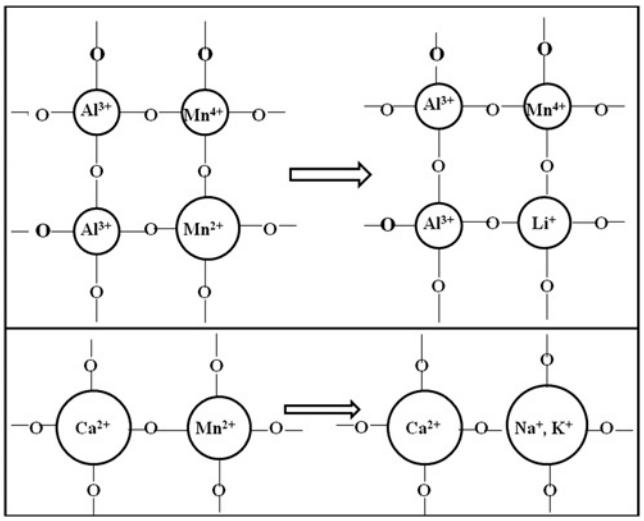

Figure 3 *Mechanisms of Mn^{2+} being replaced by alkali-chloride*

emission intensity. This phenomenon may be attributed to the matrix ion deformation after multifarious alkali-chloride doping. As illustrated in Fig. 3, firstly, the radius of Li^+ is much smaller than Mn^{2+} but closer to Mn^{4+}. It made Mn^{4+} enter into the Al^{3+} lattice more easily which could increase the number of luminous centres. It is also good for charge compensation [12]. Secondly, K^+ and Na^+ induced a variation in the local environment of the Ca^{2+} which inhibited the transformation from Mn^{4+} to Mn^{2+}. Thirdly, the lattice contraction of Mn^{4+} introduced a closer packing between the ions after the introduction of the smaller Li^+. At the same time, the anti contractile force of the O^{2-} induced an electron cloud deformation of Mn^{4+}, and in the electron cloud the cations and anions were tightly linked together to keep the structure stable. In view of this, the electrons could transit to high level with less energy and then release high energy in reverse transition, which will make a shorter wavelength and stronger fluorescence. Alkali-chloride is also reported in the literature since it has the function of the flux that will decrease the reactant synthesis temperature and improve the performance of the reaction process [13].

The XRD patterns in Fig. 4 exhibited mixed phases, which are the rhombohedral Al_2O_3 and the hexagonal $CaAl_{12}O_{19}$. Most of the peaks of $CaMAl_{12}O_{19}:Mn^{4+}$ are well matched with JCPDS Card Number 00-038-0470($CaAl_{12}O_{19}$), 00-042-1468(Al_2O_3). The samples without alkali-chloride appear to still have rhombohedral Al_2O_3 present. However, the rhombohedral Al_2O_3 phase peaks disappeared and only a single phase peak of $CaAl_{12}O_{19}$ was increased when $CaAl_{12}O_{19}:Mn^{4+}$ is doped with alkali-chloride. The remarkable enhancement in the $CaAl_{12}O_{19}$ peak is ascribed to the modification of three different alkali-chlorides for $CaAl_{12}O_{19}:Mn^{4+}$.

The hexagonal crystal system is the most compact way of accumulation. The short spaces between anion and cation could urge a severe deformation in the outermost layer of the nucleus of Mn^{4+}, leading to an emission of fluorescence light with shorter wavelength and higher luminous intensity. This means alkali metal-ion is beneficial to form hexagonal $CaAl_{12}O_{19}$. It may also be inferred that the more the kinds of alkali-chloride joined, the easier is the Mn^{4+} doped in the lattice of CAO.

Surface features of the as-prepared powder samples with and without alkali metal ions is presented in Figs. 5*a–c*, respectively. As Fig. 5*a* indicates, the powers are severely agglomerated and the sample has no uniform shapes and sizes. They could be used only by high grinding, which may reduce the luminous intensity of the power. The size of the sample generated from mixing with

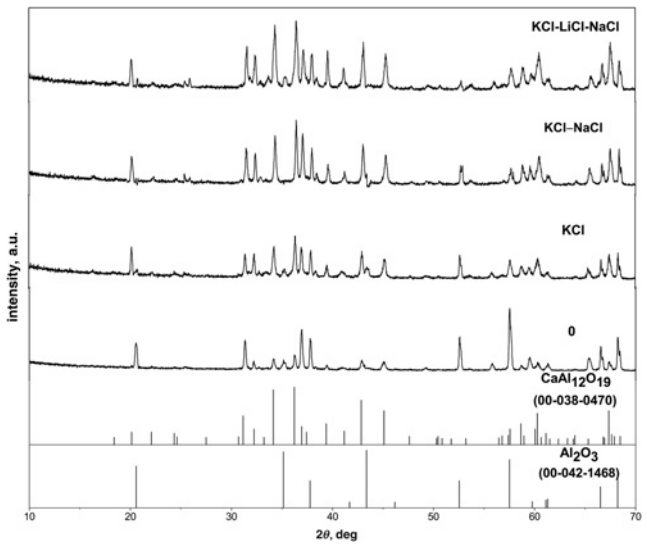

Figure 4 *XRD patterns of $CaMAl_{11.98}O_{19}:0.02Mn^{4+}$ prepared with the kinds of alkali-chloride from 0 to 3*

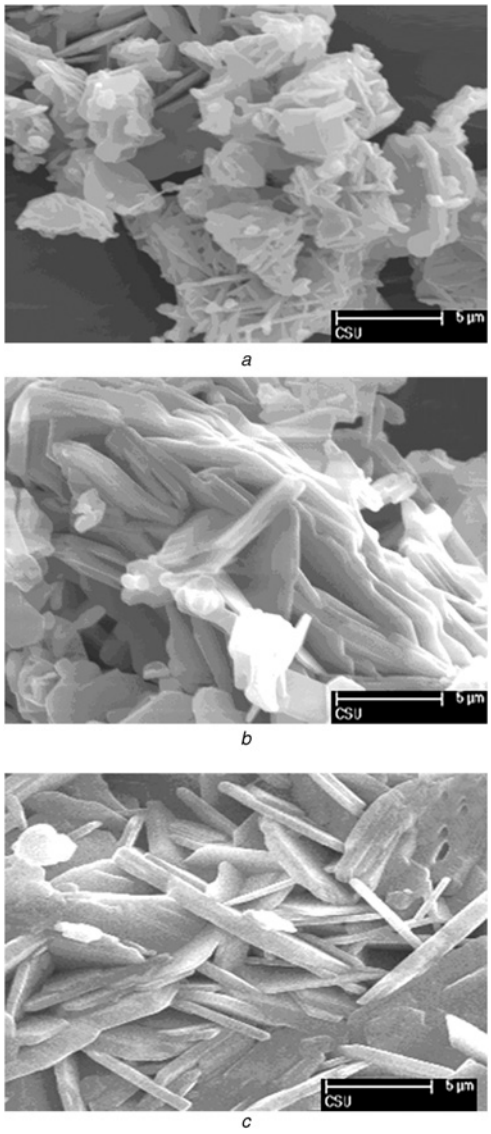

Figure 5 *SEM of $CaAl_{11.98}O_{19}:0.02Mn^{4+}$*
a Without alkali-chloride
b With KCl and LiCl
c With KCl, LiCl and NaCl

one or more kinds of alkali-chloride exhibited high-quality crystallinity and a directional polygonal structure. These results were also in good agreement with those obtained from XRD analysis. The crystallites size from SEM images of samples b and c were found to be around 5 μm, which was favourable for LED applications in white LEDs [14]. It may be mentioned that the observed features are inherent in combustion-derived powders [15].

4. Conclusions: When the Mn^{4+} concentration in CAO reached 0.02 mol, the strongest fluorescence intensity of the samples can be achieved. The use of joint doping alkali-chloride can obtain a good performance of red fluorescent material. The XRD analysis supports the Mn^{4+} substitution at Al^{3+} without disturbing the $CaAl_{12}O_{19}$ lattice. CAO:Mn led to a significant increase in luminescence intensity through incorporation of alkali-chloride cations into the lattice. Different alkali cations have different effects on the phosphor. The Mn^{4+}–M^+ pairs maintain the charge balance properly and reduce the concentration quench of Mn^{4+}, which enhances the Mn^{4+} emission. The major advantages of the synthetic process are its simplicity, high speed and low cost. Furthermore, the red phosphor was sized

doi: 10.1049/mnl.2012.0809

approximately 5–10 μm, which suggests that Mn^{4+}-doped $CaAl_{12}O_{19}$ phosphors have the potential to be used as deep red-emitting phosphors for LEDs. A fundamental understanding of the effects of cation radius on $CaMAl_{12-x}O_{19}:xMn^{4+}$ have been investigated and their dependence on the lattice environment is essential for further improving the phosphor performance and for the development of new phosphors.

5. Acknowledgments: This work was supported by Gui Zhou Province's Nature Science Foundation of China (J [2011]2077).

6 References

[1] Taguchi T.: 'Present status of white LED lighting technologies in Japan', *Light Vis. Environ*., 2003, **27**, pp. 131–133

[2] Sheu J.K., Chang S.J., Kuo C.H., *ET AL*.: 'White-light emission from near UV InGaN-GaN LED chip precoated with blue/green/red phosphors', *IEEE Photonics Technol. Lett*., 2003, **15**, pp. 18–21

[3] Zhang M., He X., Ding W.J., Wang J.: 'Oxynitride and nitride phosphors for white LEDs', *Progr. Chem*., 2010, **22**, pp. 376–383

[4] Pan Y.X., Wu M.M., Su Q.: 'Tailored photoluminescence of YAG:Ce phosphor through various methods', *J. Phys. Chem. Solids*, 2004, **65**, (5), pp. 845–849

[5] Yen W.M., Shionoya S., Yamamoto H.: 'Phosphor handbook' (CRC Press, 2006)

[6] Kemeny G., Haake C.H.: 'Activator centre in magnesium fluorogermanate phosphors', *J. Chem. Phys*., 1960, **33**, pp. 783–787

[7] Bergstein A., White W.B., Electro J.: 'Manganese-activated luminescence in $SrAl_{12}O_{19}$ and $CaAl_{12}O_{19}$', *J. Electr. Chem. Soc*., 1971, **118**, pp. 1160–1170

[8] Xu X.E.: 'The applied luminescent materials' (China Light Industry Press, Beijing, 2008, 2nd edn), pp. 166–170

[9] Pan Y.X., Liu G.K.: 'Influence of Mg^{2+} on luminescence efficiency and charge compensating mechanism in phosphor $CaAl_{12}O_{19}:Mn^{4+}$', *J. Lumin*., 2011, **131**, pp. 465–468

[10] He H., Song X.F., Fu R.L., *ET AL*.: 'Crystal structure and luminescence of $Li_2Ca_{0.7}Sr_{0.3}SiO_4:Eu^{2+}$ and its application in multi-phosphor converted white LEDs', *J. Alloys Compd*., 2010, **493**, pp. 401–405

[11] Tansel B., Sager J., Rector T.: 'Significance of hydrated radius and hydration shells on ionic permeability during nanofiltration in dead end and cross flow modes', *Sep. Purif. Technol*., 2006, **51**, pp. 40–47

[12] Brik M.G., Pan Y.X., Liu G.K.: 'Spectroscopic and crystal field analysis of absorption and photoluminescence properties of red phosphor $CaAl_{12}O_{19}:Mn^{4+}$ modified by MgO', *J. Alloys Compd*., 2011, **509**, pp. 1452–1456

[13] Yu X.B., Xu X.L., Zhou C.L., Tang J.F., Peng X.D., Yang S.P.: 'Synthesis and luminescent properties of $SrZnO_2:Eu^{3+}$, M^+ (M = Li, Na, K) phosphor', *Mater. Res. Bull*., 2006, **41**, pp. 1580–1583

[14] Kang H.G., Park J.K., Kim C.H., Choi S.C.: 'Luminescence properties of $MAl_{12}O_{19}:Mn^{4+}$ (M = Ca, Sr, Ba) for UV LEDs', *J. Ceram. Soc*., 2009, **117**, pp. 649–653

[15] Singh V., Gundu Rao T.K.: 'Studies of defects in combustion synthesized europium-doped $LiAl_5O_8$ red phosphor', *J. Solid State Chem*., 2008, **181**, (6), pp. 1387–1392